Biotechnology Journal
www.biotechnology-journal.com

Dielectrophoretic Manipulation of Janus Particle in Conductive Media for Biomedical Applications

*Minji Lee, Jong Bin Won, Dae Ho Jung, Jaekyoung Kim, Yonghyun Choi, Kubra Akyildiz, Jonghoon Choi, Kyobum Kim, Jiung Cho, Hyunsik Yoon, and Hyung-Jun Koo**

Janus particles are applied to many fields including biomedical applications. To expand the usability of Janus particles, a technique to manipulate the particle movement is required. A dielectrophoresis (DEP) method can be a promising candidate; however, independent manipulation or separation of Janus particle by DEP is still challenging. Additionally, DEP of Janus particles in conductive media is important especially for biomedical applications where ion-rich media are typically used. Here, the experimental results of DEP-induced transport and separation of the Janus particle in conductive media are presented. To predict the DEP behavior, the Clausius–Mossotti (CM) factors of both Janus and homogeneous particles are calculated, depending on the alternating current (AC) frequency and medium conductivity. The Janus particles show the positive-DEP behavior at the entire AC frequency region tested due to the metal-coated half surface. On the other hand, the homogeneous particles show the negative-DEP behavior at the high AC frequency or in conductive media. Additionally, in the conductive media, an electrohydrodynamic flow hinders the DEP-driven particle transport below MHz AC frequencies. Finally, the separation of the Janus particles from the homogeneous ones is experimentally demonstrated and the separation efficiency is discussed based on the evaluation parameters established in this study.

1. Introduction

Janus particles, a concept popularized by Pierre Gilles de Gennes in 1991, refer to the particles having two surfaces with different physicochemical properties. Janus particles have been widely used for photonic,[1–3] electronic,[4–6] catalytic,[7–9] and biomedical applications.[10–12] In particular, many biosensor studies using the anisotropic surface properties of Janus particles have been performed for the detection of biomolecules, such as viruses, proteins, glucose, DNA, and cancer cells.[13,14] Wu et al. used Janus particles to detect the tumor cells based on a surface-enhanced Raman scattering (SERS) technique.[15] The polymer region of the Janus particle adsorbs antibody which specifically binds to the BT474 cancer cell, while the metal side allows the strong SERS signal. Lu et al. developed a colorimetric glucose sensor by using hematite-silica Janus nanoparticles where one half of the Janus particle was covered by glucose oxidase (GOx).[16] To enhance the usability of Janus particles for biosensor applications, an appropriate technique to manipulate the particle transport is required, so that the Janus particles conjugated by specific bio-objects can be separated and isolated from pristine particles.

Various techniques for particle manipulation have been reported. Examples include the inertial lift force utilized in a microchannel,[17–19] ultrasonic standing wave field,[20,21] and magnetic field gradient.[22–25] Among them, techniques that practice on the electric field such as electrophoresis (EP)[26] and dielectrophoresis (DEP) have been predominantly used. It is because an electrical field can provide a fast switching of the exerted force on particles in addition to the control ability of applied force magnitude and direction. DEP, defined by Pohl in 1951,[27] refers to a transport phenomenon, resulting from a directional force applied on a dielectric particle when it is in an uneven electric field. Unlike EP, which can only be applied to charged particles, DEP has the advantage that it can be applied to almost all particles as it uses the polarization of the substance. Therefore, it can be adjusted for the motion control and separating operations of various particles, ranging from synthetic organic/inorganic particles to

M. Lee, J. B. Won, D. H. Jung, J. Kim, K. Akyildiz, Prof. H. Yoon, Prof. H.-J. Koo
Department of Chemical and Biomolecular Engineering
Seoul National University of Science and Technology
232 Gongneung-ro, Seoul 01811, Republic of Korea
E-mail: hjkoo@seoultech.ac.kr
Y. Choi, Prof. J. Choi
School of Integrative Engineering
Chung-Ang University
84 Heukseok-ro Seoul 06974, Republic of Korea
Prof. K. Kim
Department of Chemical and Biochemical Engineering
Dongguk University
Pildong-ro 1-gil Seoul 04620, Republic of Korea
Dr. J. Cho
Western Seoul Center
Korea Basic Science Institute
150 Bugahyeon-ro Seoul 03759, Republic of Korea

The ORCID identification number(s) for the author(s) of this article can be found under https://doi.org/10.1002/biot.202000343

DOI: 10.1002/biot.202000343

biomolecules, such as protein,[28–30] virus,[31–33] bacteria,[34–36] and cells.[37–39]

Previously, the DEP behavior of Janus particles has been studied. Gangwal et al. demonstrated the assembly of Janus particles under an alternative current (AC) electric field at the frequency higher than 10 kHz.[40] The Janus particles are assembled to form a staggered chain structure while the metal-coated halves align along the electric field direction. They also confirmed that the staggered chain structure is the most favorable orientation of particles by performing a numerical simulation of the electric energy of the system. Zhang et al. investigated the colloidal assembly structure of Janus particles depending on the conductivity of medium under high frequency, non-uniform AC electric field.[41] At low medium conductivity ($\sigma_m = 0.0007$–0.0153 S m^{-1}) and wide AC frequency range (25 kHz to 20 MHz), pearl chains of Janus particles are formed due to the dominant DEP-induced particle assembly. On the other hand, at high medium conductivity ($\sigma_m = 0.0153$–0.116 S m^{-1}), the particle chaining is disturbed because of the induced-charge electrophoresis (ICEP) along with DEP.

Independent manipulation or separation of Janus particle in a particle mixture by DEP is still challenging. Zhao and Li performed a simulation study of the DEP behavior of homogeneous polystyrene (PS) particles and Janus particles in a nano-orifice based microfluidic chip where the direct current (DC)-based microfluidic chip could enable the separation of Janus particle from a particle mixture with different types or sizes of particles.[42] Furthermore, the DC–DEP behavior was systematically investigated depending on the coating coverage, thickness, and material of the metal side of the Janus particle. However, Janus particle separation from the particle mixture has not been experimentally shown yet. Additionally, the 180 V of DC voltage used in the simulation work, is probably less practical because of the safety issue or occurrence of a severe electrochemical reaction. Determination of the DEP behavior of particles in conductive media is also critical especially for the bio-related applications where the experiment is primarily performed in conducting media, such as buffer solutions.

In this paper, we discuss the DEP behavior of Janus particles depending on medium conductivity and present an experimental study of their separation from homogeneous particles in conductive media. Janus particles were prepared by transferring the particle monolayer from an air/water interface onto a substrate, followed by the anisotropic deposition of metal. DEP behavior of the Janus particles is investigated at various medium conductivity and AC frequencies. To predict the DEP behavior, the Clausius–Mossotti (CM) factor and the electric field distribution around the electrode were calculated. The electrothermal effect, which is an additional transport phenomenon in a conductive medium under the electric field, is discussed. Subsequently, the DEP behavior of the homogeneous PS particle with a single surface property is investigated and compared to that of the Janus particle. Finally, the DEP behavior of the mixed suspension of the Janus particles and the homogeneous particles is observed, and the optimum DEP conditions for the efficient separation of the Janus particle are discussed based on the quantitative parameters established in this study.

2. Results and Discussion

2.1. CM Factor and DEP Behavior of Janus Particles

The time-averaged DEP force on a spherical particle can be calculated by the following equation

$$F_{\mathrm{DEP}} = 2\pi\epsilon_{\mathrm{m}} r^3 \mathrm{Re}\left[f_{\mathrm{CM}}\right] \nabla\left|E_{\mathrm{rms}}\right|^2 \tag{1}$$

where ϵ_{m} is the permittivity of the medium, r is the particle radius, E_{rms} is the root-mean-square electric field, and Re[f_{CM}] is the real part of the CM factor that is related to the effective polarizability of the particle. The CM factor is a complex number that is defined by

$$f_{CM} = \frac{\epsilon_p^* - \epsilon_m^*}{\epsilon_p^* + 2\epsilon_m^*} \tag{2}$$

$$\epsilon_p^* = \epsilon_0\epsilon_p - j\frac{\sigma_p}{\omega},\ \epsilon_m^* = \epsilon_0\epsilon_m - j\frac{\sigma_m}{\omega} \tag{3}$$

where ϵ_{p}^* and ϵ_{m}^* are the complex permittivity of particle and medium, ϵ_0 is the permittivity of free space (8.854×10^{-12} F m^{-1}), σ_{p} and σ_{m} are conductivity of particle and medium, respectively, and ω is the angular frequency ($\omega = 2\pi f$) of the applied AC field. As a result, the CM factor depends on the applied AC frequency, permittivity, and conductivity of media and particles. The sign of Re[f_{CM}] determines the direction of the DEP force, i.e., p-DEP or n-DEP. When Re[f_{CM}] is positive or negative, the particle moves toward to or pushed out of the dense electric field region. The DEP force is also proportional to the magnitude of Re[f_{CM}]. The Re[f_{CM}] value of Janus particles can be obtained from the equation below

$$Re\left[f_{\mathrm{CM,Janus}}\right] = \frac{1}{2}\times\left[\left(Re[f_{\mathrm{CM,\ PSparticle/Cr/Au}}]\right) + \left(Re[f_{\mathrm{CM,homogeneous}}]\right)\right] \tag{4}$$

where (Re[$f_{\mathrm{CM,PS\ particle/Cr/Au}}$]) means homogeneous PS particles coated with metals Cr and Au, and (Re[$f_{\mathrm{CM,homogeneous}}$]) means homogeneous PS particles without a metal coating.

To predict the DEP behavior of Janus particles in media with different conductivity, Re[f_{CM}] was calculated as a function of AC frequency ($f = 10^4$ Hz to 10 MHz) in deionized (DI) water, 0.1×10^{-3} M NaCl, and 3.8×10^{-3} M NaCl solutions (**Figure 1**A). The Janus particle is expected to exhibit the p-DEP behavior since its Re[f_{CM}] values are positive for the entire frequency range in DI water ($\sigma_m = 5.5 \times 10^{-6}$ S m^{-1}). Re[f_{CM}] value stays almost constant at unity up to the hundreds of kHz but drastically decreases starting from 1 MHz to higher frequency. At the frequency above 10 MHz, Re[f_{CM}] converges to about 0.3. The permittivity and conductivity values of the materials used for the numerical calculations are shown in Table S1 (Supporting Information). Thus, it is expected that p-DEP behavior is strong in the frequency region below 1 MHz and becomes weaker in the frequency region above 1 MHz. In NaCl media, there is little change in the Re[f_{CM}] value

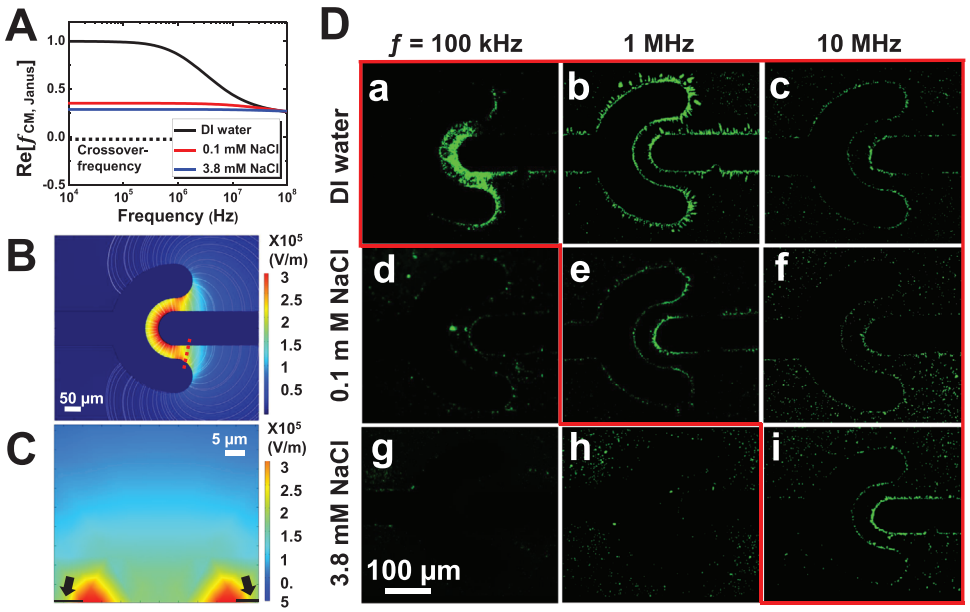

Figure 1. A) CM factors of the Janus particles depending on AC frequency in different media (DI water, 0.1×10^{-3} M NaCl, 3.8×10^{-3} M NaCl). 2D simulation results of the distribution and streamlines of the electric field around of the electrodes under AC voltage of V_{pp} = 10 V: B) top-view and C) side-view. The dotted line in (B) indicates the position for (C). The black arrows in (C) designate the electrodes. D) Distribution of Janus particles in DI water, 0.1×10^{-3} M NaCl, and 3.8×10^{-3} M NaCl media at various AC frequencies. V_{pp} = 10 V. All images were taken after 10 min of the AC field application. The p-DEP behavior of Janus particles is observed in the box by the red lines.

with the frequency. Throughout the frequency range employed in this study (10^4 Hz to 10 MHz), the calculated Re[$f_{CM,}$] values are almost constant at ≈0.3 and ≈0.25 in 0.1×10^{-3} M NaCl (σ_m = 0.01 S m^{-1})[43] and 3.8×10^{-3} M NaCl (σ_m = 0.05 S m^{-1}),[44] respectively. The Re[f_{CM}] of Janus particles in a more conductive NaCl solution is much lower than that in DI water. Consequently, based on the calculated Re[f_{CM}] values, it is expected that the Janus particles exhibit p-DEP behavior in all conditions of medium conductivity and AC frequency used in the study. Also, the p-DEP behavior of Janus particles at the AC frequency up to 10 MHz would be more significant in DI water than in more conductive salt solutions.

To predict the electric field distribution around the designed electrode, the computational simulation was performed (Figure 1B,C). For the top-view result, the strong field gradient is formed at the gap between the two electrodes whereas, for the side-view result, the sharper gradient of the electric field is shown at the edge of the electrodes. Based on the simulation results, particles affected by p-DEP force are expected to be collected at the gap between the electrodes as well as the edges of each electrode. The p-DEP driven transport toward the electrode edges is probably stronger due to the sharper gradient of the electric field.

The DEP-driven transport of the Janus particles, depending on the medium conductivity and AC frequency was experimentally observed (Figure 1D) and was compared to what was expected based on the calculated Re[f_{CM}] values and the simulation results. For all cases in Figure 1D, the transport and collection of the particles were nearly equilibrated within 10 min. No significant aggregation of the Janus particles driven by van der Waals interaction has been observed in any media conditions. At the frequency of 100 kHz in DI water, the Janus particles are collected at the gap between the two electrodes as well as the edges of the electrodes (Figure 1Da). This is in good agreement with p-DEP behavior expected. As the frequency increases above 1 MHz, the number of the collected Janus particles decreases, and the particles are collected only at the electrode edges, as shown in Figure 1Dc. This is because the Re[$f_{CM,Janus}$] drastically decreases above 1 MHz (Figure 1A), resulting in the weak p-DEP force. In 0.1×10^{-3} and 3.8×10^{-3} M NaCl solutions, the Janus particles are also collected at the electrode edges at above 1 MHz (Figure 1De,f) and above 10 MHz (Figure 1Di), respectively, by the p-DEP force. Interestingly, no significant collection of the Janus particles is observed in 0.1×10^{-3} and 3.8×10^{-3} M NaCl solutions at relatively low AC frequencies (Figure 1Dd,g,h). We hypothesize that this may be due to the convective flow of the medium fluid driven by an additional transport phenomenon under the AC field, which is an electrothermal effect.

2.2. Effect of the Electrothermal Flow (ETF) on the DEP Behavior of Particles

ETF, a well-known phenomenon in electrohydrodynamics, is caused by electrothermal forces acting on the bulk fluid in the presence of the electrical conductivity and permittivity gradients in electrolyte solutions due to the temperature gradient.[44] The temperature gradient formed by Joule heating leads to the gradient in many physical properties, such as permittivity, conductivity, density, and viscosity which drive the net flow of surrounding media. The AC electric fields that are used in DEP based microdevices can cause local heating around electrodes, which generates volume forces in the liquid by producing gradients in conductivity and permittivity.[45] The temperature gradient in the experimental setup was confirmed by the Joule

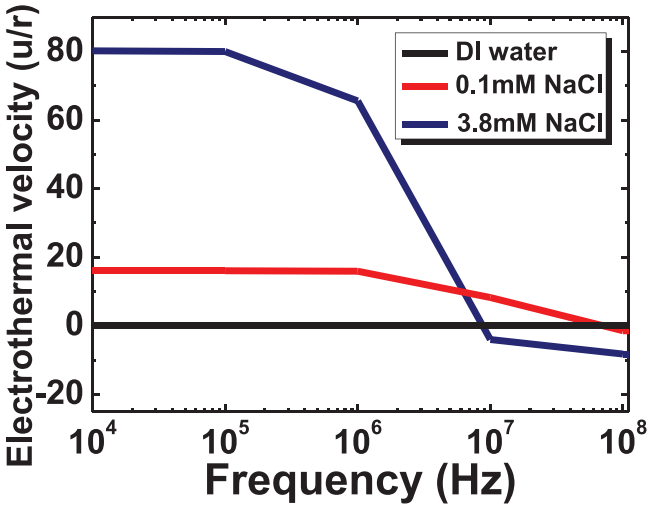

Figure 2. Electrothermal velocity depending on AC frequency in different media.

heating simulation (Figure S3, Supporting Information). The equation for the maximum electrothermal velocity of the flow generated by ETF, $u_{\mathrm{ETH,max}}$, is given by

$$u_{\mathrm{ETH,max}} = \frac{1}{192\pi^2}\,\frac{M}{T}\,\frac{\varepsilon\sigma V^4}{k\mu r_{\mathrm{ETH}}} \tag{5}$$

where ϵ, σ, k, and μ are the permittivity, the electrical conductivity, the thermal conductivity, and the viscosity of the fluid (medium), respectively. V is the applied voltage, r_{ETH} is the characteristic length for ETF, and M is the electrothermal factor (M factor), which is given by

$$M = \frac{(\beta-\alpha)\,T}{1+\left(\frac{\omega\epsilon}{\sigma}\right)^2} + \frac{1}{2}\alpha T \tag{6}$$

$$\alpha = (\partial\varepsilon/\partial T)/\varepsilon, \beta = (\partial\sigma/\partial T)/\sigma \tag{7}$$

where ω is the radian frequency. M factor determines the direction and flow velocity of the ETF. According to Equation (6) when the temperature, conductivity of the medium, and permittivity are constant, M factor, which is a function of frequency, is between –0.7 and 7. α and β are represented by Equation (7), while for aqueous solutions with moderate concentration (≈1 M), $\alpha = -0.4\%\ \mathrm{K}^{-1}$ and $\beta = 2.0\%\ \mathrm{K}^{-1}$ can be used.[46]

Figure 2 shows the ETF velocity depending on medium conductivity and AC frequency, calculated by Equations (5) and (6). In DI water, the ETF effect is negligible regardless of frequency, due to the low medium conductivity. In conductive media of NaCl solutions, the ETF effect becomes meaningful and its velocity tends to decrease with increasing frequency. In a 0.1×10^{-3} M NaCl medium, ETF is expected to form up to 1 MHz frequency, above which the ETF velocity rapidly decreases. In 3.8×10^{-3} M NaCl medium, ETF becomes more significant up to 10 MHz frequency. Such an ETF phenomenon in conductive media presumably hinders the particle collection by DEP at AC frequency below 1 MHz, which is well-matched with the experimental results in Figure 2 Indeed, at frequencies below 100 kHz, the significant convective transport of the particles has been observed, presumably due to the enhanced ETF.

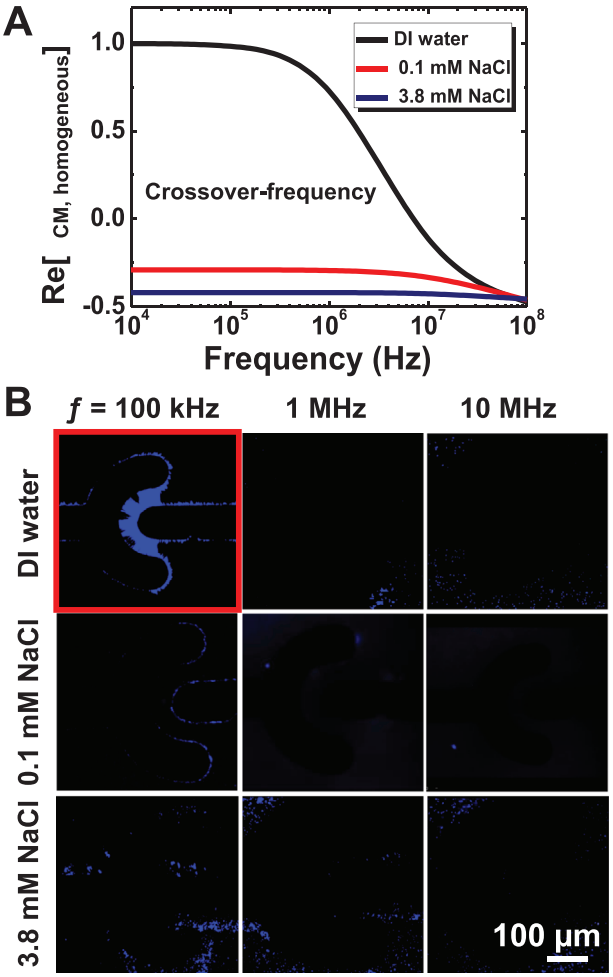

Figure 3. A) CM factors of the homogeneous PS particles depending on AC frequency in different media (DI water, 0.1×10^{-3} M NaCl, and 3.8×10^{-3} M NaCl). B) Distribution of homogeneous PS particles in DI water, 0.1×10^{-3} M NaCl, and 3.8×10^{-3} M NaCl at various AC frequencies. V_{pp} = 10 V_{pp}. All images were taken after 10 min of the AC field application. The p-DEP behavior of Janus particles is observed in the box by the red lines.

2.3. CM Factor and DEP Behavior of Homogeneous PS Particles

For the separation of the Janus particle from the homogeneous particle by using DEP force, the CM factor, and the DEP behavior of homogeneous PS particles should also be investigated. **Figure 3**A shows the calculated values of Re[f_{CM}] in media with different conductivity. In DI water, Re[f_{CM}] value is almost constant up to the frequency of 100 kHz and then becomes negative at the frequency above 5 MHz. Therefore, the DEP force direction is expected to switch around the MHz frequency region. On the other hand, in more conductive media of 0.1×10^{-3} M NaCl and 3.8×10^{-3} M NaCl, Re[f_{CM}] is negative (between –0.25 and –0.5) through all frequency ranges, implying the n-DEP behavior of the particles.

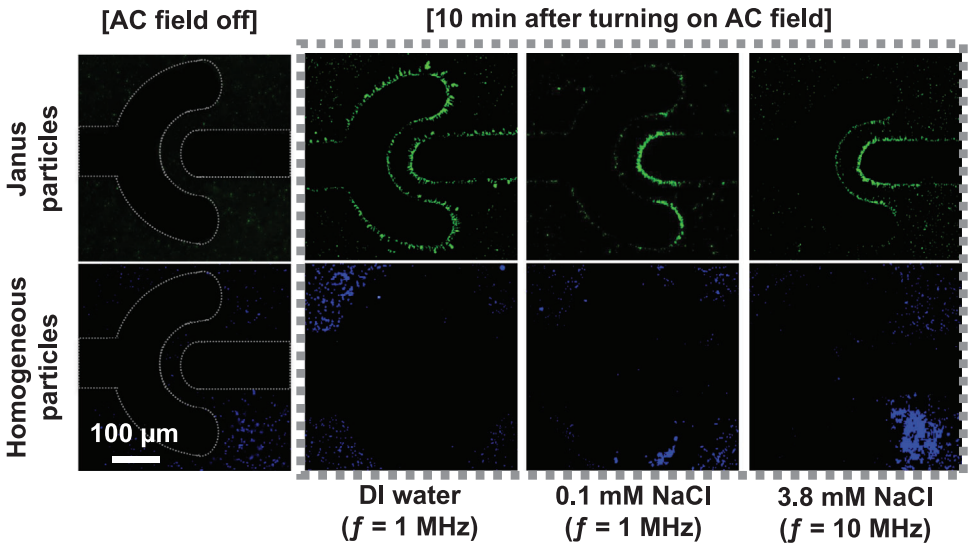

Figure 4. Particle distribution of Janus particles ($\lambda_{em} \approx 505$ nm) and homogeneous PS particles ($\lambda_{em} \approx 407$ nm) in a mixed suspension by DEP at the selected AC frequencies. High contrast figures and more data at various AC frequencies are shown in Figures S4–S7 of the Supporting Information. The particle number ratio in the mixed suspension is ≈1:1 (Janus particles:homogeneous PS particles).

Transport of the homogeneous PS particles by DEP was experimentally observed in various media with different conductivity (Figure 3B . In the case of DI water, particles were effectively collected at the gap of the two electrodes at 100 kHz AC frequency, while they were pushed out of the electrode gap at the frequency above 1 MHz. The result is in accordance with the expected DEP behavior from the calculated Re[f_{CM}] value in Figure 3A From the Re[f_{CM}] calculation, n-DEP behavior was predicted at the frequency higher than 5 MHz; however, the actual experiment showed n-DEP behavior even at the lower frequency of 1 MHz. This is possible because of the increase in the conductivity of DI water. For example, carbon dioxide from air is likely to be dissolved into the DI water. Moreover, impurity, e.g. surfactant from the commercial particle suspension, could be present in the media. Such impurity ions or molecules possibly increase the conductivity of the DI water medium, which may decrease the frequency where DEP direction switches. In NaCl media, n-DEP transport of the homogeneous PS particles is dominant at all the frequencies tested, as expected by the CM factor values calculated. Also, the ETF-induced circulation of particles was observed near the electrode at the frequency of 100 kHz.

2.4. DEP Separation of a Janus/Homogeneous Particle Mixture

Since Janus and homogeneous PS particles show different DEP behaviors depending on the frequency and conductivity of media, these two particles in a mixed suspension could be separated by using DEP force. From the previous result, separation would be possible in the MHz frequency region where ETF is minimized and Janus particles and homogeneous PS particles have opposite DEP behaviors. **Figure 4** shows the distribution of respective particles under AC frequencies selected for efficient separation. As expected, under the DEP conditions in Figure 4 the Janus particles are selectively collected at the electrode edges and at the gap between the electrodes which indicates their p-DEP behavior, whereas the homogeneous particles are pushed away from the electrodes and dispersed in the medium, by the n-DEP behavior.

For the quantitative evaluation of DEP separation, we defined a numerical parameter by Equation (8)

$$\text{Separation selectivity (\%)} = \left(\frac{\text{Number of the Janus particles among the ones collected}}{\text{Number of the particles collected}} - 0.5\right) \times 200 \quad (8)$$

From the equation, the "separation selectivity" has values ranging from –100% to 100%. "–100%" and "100%" mean that all the particles collected are homogeneous PS particles and Janus particles, respectively. When the numbers of Janus particles and homogeneous particles collected are the same, separation selectivity becomes zero, which means no selectivity. The number of collected Janus particles was calculated using the Image J program, which was calculated by dividing the total area of particles collected by the area of one particle. It is assumed that the particles are no longer collected after 10 min of the voltage application. The Janus particle size is 1 μm and the electrode thickness is ≈100 nm, so it is assumed that the particles only form a monolayer while being collected by DEP force.

Figure 5 shows the number of Janus particles collected by p-DEP and the separation selectivity. In the case of DI water, more Janus particles are collected at lower frequencies, while separation selectivity increases as the frequency increases. For the DI water medium, about 11 000 particles were collected at 100 kHz, but the separation selectivity is as low as –16%. The reason is that both Janus and homogeneous particles are captured by p-DEP at 100 kHz. At 1 MHz, about 4200 Janus

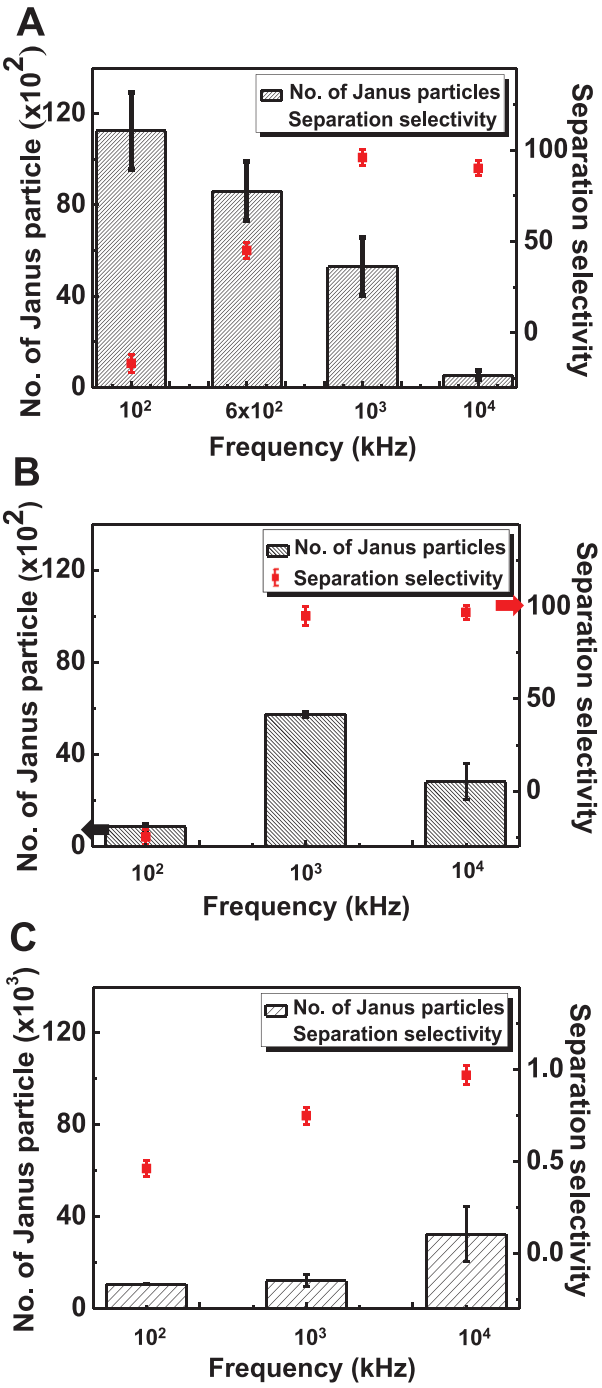

Figure 5. The number of Janus particles collected and the separation selectivity depending on the AC frequencies in different media: A) DI water, B) 0.1×10^{-3} M NaCl, and C) 3.8×10^{-3} M NaCl. The mixed particle suspension injected contains approximately 100 000 particles per 1.3 cm^2 with about 1:1 Janus/homogeneous PS particle ratio.

particles were collected and the separation selectivity is 98%. At 10 MHz, the number of Janus particles collected drastically decreased to 1300, but the separation selectivity stays above 95%. As the frequency increases, the value of separation selectivity increases because only the Janus particles are collected around the electrodes by p-DEP, and most of the homogeneous particles are pushed out of the electrodes by n-DEP. In conductive media of NaCl solutions, the separation selectivity increases with AC frequency similar to that in DI water while the number of collected particles at 100 kHz is significantly low due to the ETF effect. The numbers of Janus particles collected on the electrode edges at 100 kHz are less than 2000 in both NaCl solutions. In the 0.1×10^{-3} M NaCl solution, the largest number of Janus particles collected is ≈6000 at 1 MHz with ≈95% separation selectivity. In the 3.8×10^{-3} M NaCl medium, since the ETF effect is influential up to 1 MHz, the number of particles collected is highest at 10 MHz. Thus, the Janus particles can be effectively separated in a mixed suspension by DEP force. For an efficient separation, the AC frequency needs to be carefully tuned depending on the medium conductivity and, in general, the AC frequency above 1 MHz is favored for better selectivity by minimizing the ETF effect.

3. Conclusion

In summary, we experimentally demonstrate the separation of the Janus particle from the homogeneous one in conductive media by using AC based-DEP technique. We investigated the DEP-driven transport of the Janus particles by calculating the CM factors at different medium conductivity and comparing them with the experimental results. To examine the effect of the medium conductivity on the DEP of particles, the media varied from DI water to ion-conductive salt solution. In DI water, the p-DEP behavior of the Janus particles is observed regardless of the AC frequency. In conductive media, however, the capture of the Janus particles by p-DEP is observed only at the high-frequency region above 1 MHz. It is theoretically revealed that, in conductive media, the ETF induced by local Joule heating becomes significant below the MHz frequency region, which disturbs the DEP-driven particle transport. For the homogenous PS particles, it is confirmed that the n-DEP behavior is shown at the high AC frequency above ≈1 MHz. Finally, the DEP technique has been applied to the separation of the Janus particle from the normal homogenous one in conductive media. The particle separation can be quantitatively analyzed depending on medium conductivity and AC frequency, by defining a new evaluation parameter of the separation selectivity. It is found that the AC frequency in a DEP system should be carefully adjusted depending on the medium conductivity, for better concentration of the Janus particles as well as higher separation selectivity. Especially, in conductive media such as a buffer solution which is widely used in bio-applications, the ETF effect should be considered and minimized. Furthermore, the separated Janus particles can be separately collected, for example, by employing a microfluidic technique. These findings could provide useful information for DEP-based manipulation of Janus particles for detection and separation of biomolecules.

4. Experimental Section

Preparation of Janus Particles: For the Janus particle preparation, fluorescent yellow–green latex beads (diameter = 1.0 μm; fluorescence $\lambda_{ex} \approx 470$ nm; $\lambda_{em} \approx 505$ nm, carboxylate-modified) were purchased in

an aqueous suspension from Sigma-Aldrich, Korea. For the homogenous PS particle preparation, Fluoresbrite BB latex beads (diameter = 1.0 μm; fluorescence $\lambda_{ex} \approx 360$ nm; $\lambda_{em} \approx 407$ nm, carboxylate-modified) were purchased in an aqueous suspension from Polysciences, Inc., Korea.

The schematic structure of the Janus particles is shown in Figure S1A (Supporting Information). The Janus particles were prepared by forming a self-assembled monolayer of homogeneous PS particles at the water–air interface and depositing a metal thin film.[47] The PS particle suspension was initially concentrated by centrifuging at 10 000 rpm for 10 min and washed with ultrapure Milli-Q water (Direct-Q 3UV, 18.2 MΩ). The aqueous colloidal suspensions which are typically 5 wt.%, were diluted with ethanol (volume ratio, PS suspension:ethanol = 1:1) to facilitate the spreading of colloidal dispersion. A hydrophilic slide glass (≈76 × 26 × 1 mm, Paul Marienfeld GmbH & Co. KG, Germany) was partially immersed in the water-filled beaker at an inclination angle of ≈45° with respect to the water surface. Sodium dodecyl sulfate (SDS) (≥98.5% (GC), Sigma-Aldrich) was added to the DI water by $\approx 0.3 \times 10^{-3}$ M to help the direct crystallization process.

When the colloidal dispersion was dropped into the slide glass by about 10 μL, a colloidal monolayer formed at the water–air interface as the particles spread. By carefully dipping a hydrophilic silicon wafer into the beaker containing the monolayer and carefully pulling it out, the PS particle monolayer was transferred on the wafer and was dried at room temperature. The half side of the dried particle monolayer on the wafer was coated with 20 nm of chrome (Cr) and 20 nm of gold (Au), sequentially, by an e-beam evaporator (ULVAC Inc, Japan). This process results in the formation of Janus microspheres where the half side is covered with a conductive Cr and Au layer. The wafer with the Janus particle monolayer was placed in a 0.03×10^{-3} M SDS aqueous solution and was sonicated in the ultrasonic bath (Hwashin power sonic 505, 40 kHz, Korea), to obtain a Janus particle suspension. The concentration of Janus particle suspension was measured by the CytoFLEX Flow Cytometry Analyzer (Beckman Coulter Inc., Korea). The prepared Janus particles, observed by scanning electron microscope (SEM, SU8010, Hitachi High Technologies Corporation, Japan), are shown in Figure S1B (Supporting Information).

Fabrication of the Experimental Setup for DEP Observation: The schematic of the DEP experimental setup is shown in Figure S2 (Supporting Information). The metal electrode was fabricated on the glass substrate by photolithographic patterning, a selective metal deposition, and a lift-off process. A positive photoresist AZ 5214E (Merch KGaA, Darmstadt, Germany) was deposited onto a slide glass, which was then spin-coated at 2000 rpm for 30 s. After coating, the soft-baking process was conducted to remove the solvent and enhance the adhesion of photoresist to the substrate. The photomask was placed on the soft-baked photoresist, which was exposed to the UV light source ($\lambda = 365$ nm, 30 mW cm^{-2}, Mask Aligner MDA-400M, MIDAS system, Korea) for 35 s. The UV-degraded region of the photoresist film was removed by using a developer (AZ 300 MIR developer, Merck, Germany). To form metal electrodes, 5 nm of titanium and 100 nm of platinum were deposited on the glass substrate with the patterned photoresist by sputtering. After the metal deposition, the substrate was immersed in acetone (Daejung, Korea) to wash off the remaining photoresist layer, resulting in the formation of the patterned electrodes.

A spacer (CoverWell Incubation chamber, 0.5 mm depth, Grace biolabs, USA) was placed on the substrate with the patterned electrodes. The Janus and the PS suspensions (≈70 μL) were separately poured into the spacer and then covered with the slide glasses to form a closed microchamber system. Electric field distribution near the microelectrodes was simulated by using the COMSOL Multiphysics simulation package (ver. 5.4, COMSOL Inc., Burlington, MA, USA). AC electric field was applied with a varied frequency ranging from 100 kHz to 10 MHz by using a function generator (Agilent 33511B, Agilent Technologies, Co.). The DEP behavior and separation of the particles in the chamber were observed by using an optical microscope (KI2000F, Optinity, Korea Lab Tech, Korea).

Supporting Information

Supporting Information is available from the Wiley Online Library or from the author.

Acknowledgements

The authors gratefully acknowledge the support provided by the Basic Science Research Program (NRF-2018R1C1B6002787) and Nano-Material Technology Development Program (No. 2017M3A7B8061942) through the National Research Foundation of Korea funded by the Ministry of Science and ICT.

Data Availability Statement

The data that support the findings of this study are available from the corresponding author upon reasonable request.

Conflict of Interest

The authors declare no conflict of interest.

Author Contributions

Hyung Jun Koo assisted in conceptualization, funding acquisition, investigation, supervision, writing original draft, and writing review and editing. Minji Lee assisted in investigation, methodology, and writing original draft. Jong Bin Won assisted in investigation and methodology. Dae Ho Jun assisted in investigation and methodology. Jaekyoung Kim assisted in formal analysis. Yonghyun Choi assisted in resources. Kubra Akyildiz assisted in resources and writing original draft. Jonghoon Choi assisted in resources. Kyobum Kim assisted in resources. Jiung Cho assisted in methodology and resources. Hyun-Sik Yoon assisted in formal analysis.

Keywords

AC frequency, dielectrophoresis, electrothermal effect, Janus particles, medium conductivity

Received: August 5, 2020
Revised: October 14, 2020
Published online: November 1, 2020

[1] S. Nedev, S. Carretero-Palacios, P. Kühler, T. Lohmüller, A. S. Urban, L. J. Anderson, J. Feldmann, *ACS Photonics* **2015**, *2*, 491.
[2] Z. Yu, C. F. Wang, L. Ling, L. Chen, S. Chen, *Angew. Chem. Int. Ed.* **2012**, *51*, 2375.
[3] Y. Zhao, H. Gu, Z. Xie, H. C. Shum, B. Wang, Z. Gu, *J. Am. Chem. Soc.* **2013**, *135*, 54.
[4] D. Suzuki, H. Kawaguchi, *Colloid Polym. Sci.* **2006**, *284*, 1471.
[5] Y. Komazaki, H. Hirama, T. Torii, *J. Appl. Phys.* **2015**, *117*, 154506.
[6] T. Nisisako, T. Torii, T. Takahashi, Y. Takizawa, *Adv. Mater.* **2006**, *18*, 1152.
[7] A. Kirillova, C. Schliebe, G. Stoychev, A. Jakob, H. Lang, A. Synytska, *ACS Appl. Mater. Interfaces* **2015**, *7*, 21218.
[8] J. Faria, M. P. Ruiz, D. E. Resasco, *Adv. Synth. Catal.* **2010**, *352*, 2359.
[9] X. Ma, K. Hahn, S. Sanchez, *J. Am. Chem. Soc.* **2015**, *137*, 4976.
[10] M. Yoshida, K. H. Roh, S. Mandal, S. Bhaskar, D. Lim, H. Nandivada, J. Lahann, *Adv. Mater.* **2009**, *21*, 4920.

[11] S. Yang, F. Guo, B. Kiraly, X. Mao, M. Lu, K. W. Leong, T. J. Huang, *Lab Chip* **2012**, *12*, 2097.
[12] S. Hwang, J. Lahann, *Macromol. Rapid Commun.* **2012**, *33*, 1178.
[13] B. Li, M. Wang, K. Chen, Z. Cheng, G. Chen, Z. Zhang, *Macromol. Rapid Commun.* **2015**, *36*, 1200.
[14] J. Reguera, H. Kim, F. Stellacci, *Chimia* **2013**, *67*, 811.
[15] L. Y. Wu, B. M. Ross, S. Hong, L. P. Lee, *Small* **2010**, *6*, 503.
[16] C. Lu, X. Liu, Y. Li, F. Yu, L. Tang, Y. Hu, Y. Ying, *ACS Appl. Mater. Interfaces* **2015**, *7*, 15395.
[17] A. A. S. Bhagat, S. S. Kuntaegowdanahalli, I. Papautsky, *Microfluid. Nanofluid.* **2009**, *7*, 217.
[18] S. S. Kuntaegowdanahalli, A. A .S. Bhagat, G. Kumar, I. Papautsky, *Lab Chip* **2009**, *9*, 2973.
[19] J. S. Park, S. H. Song, H. I. Jung, *Lab Chip* **2009**, *9*, 939.
[20] Y. Liu, K. M. Lim, *Lab Chip* **2011**, *11*, 3167.
[21] A. Nilsson, F. Petersson, H. Jönsson, T. Laurell, *Lab Chip* **2004**, *4*, 131.
[22] E. Furlani, *J. Phys. D Appl. Phys.* **2007**, *40*, 1313.
[23] K. H. Han, A. Bruno Frazier, *J. Appl. Phys.* **2004**, *96*, 5797.
[24] J. Jung, K. H. Han, *Appl. Phys. Lett.* **2008**, *93*, 223902.
[25] H. Fatima, K. S. Kim, *Korean. J. Chem. Eng.* **2017**, *34*, 589.
[26] F. C. Huang, C. S. Liao, G. B. Lee, *Electrophoresis* **2006**, *27*, 3297.
[27] H. A. Pohl, *J. Appl. Phys.* **1951**, *22*, 869.
[28] T. Honegger, D. Peyrade, *Biomicrofluidics* **2012**, *6*, 044115.
[29] A. Nakano, F. Camacho-Alanis, T. C. Chao, A. Ros, *Biomicrofluidics* **2012**, *6*, 034108.
[30] A. Nakano, A. Ros, *Electrophoresis* **2013**, *34*, 1085.
[31] M. P. Hughes, H. Morgan, F. J. Rixon, J. P. Burt, R. Pethig, *Biochim. Biophys. Acta, Gen. Subj.* **1998**, *1425*, 119.
[32] H. Maruyama, K. Kotani, T. Masuda, A. Honda, T. Takahata, F. Arai, *Microfluid. Nanofluid.* **2011**, *10*, 1109.
[33] A. Sonnenberg, J. Y. Marciniak, J. McCanna, R. Krishnan, L. Rassenti, T. J. Kipps, M. J. Heller, *Electrophoresis* **2013**, *34*, 1076.
[34] R. Hamada, H. Takayama, Y. Shonishi, L. Mao, M. Nakano, J. Suehiro, *Sens. Actuators B Chem.* **1996**, *181*, 439.
[35] G. H. Markx, P. A. Dyda, R. Pethig, *J. Biotechnol.* **1996**, *51*, 175.
[36] A. Sanchis, A. Brown, M. Sancho, G. Martinez, J. Sebastian, S. Munoz, J. Miranda, *Bioelectromagnetics* **2007**, *28*, 393.
[37] M. Alshareef, N. Metrakos, E. Juarez Perez, F. Azer, F. Yang, X. Yang, G. Wang, *Biomicrofluidics* **2013**, *7*, 011803.
[38] S. Bhattacharya, T. C. Chao, N. Ariyasinghe, Y. Ruiz, D. Lake, R. Ros, A. Ros, *Anal. Bioanal. Chem.* **2014**, *406*, 1855.
[39] H. Song, J. M. Rosano, Y. Wang, C. J. Garson, B. Prabhakarpandian, K. Pant, E. Lai, *Lab Chip* **2015**, *15*, 1320.
[40] S. Gangwal, O. J. Cayre, O. D. Velev, *Langmuir* **2008**, *24*, 13312.
[41] L. Zhang, Y. Zhu, *Langmuir* **2012**, *28*, 13201.
[42] K. Zhao, D. Li, *J. Micromech. Microeng.* **2017**, *27*, 095007.
[43] B. Liao, L. Wei, Z. Chen, X. Guo, *RSC Adv.* **2017**, *7*, 15060.
[44] S. Park, M. Koklu, A. BeskoK, *Anal. Chem.* **2009**, *81*, 2303.
[45] D. Chen, H. Du, *J. Micromech. Microeng.* **2006**, *16*, 2411.
[46] D. R. Lide, *CRC Handbook of Chemistry and Physics: A Ready-Reference Book of Chemical and Physical Data*, **1995**, CRC Press, Boca Raton, FL.
[47] N. Vogel, S. Goerres, K. Landfester, C. K. Weiss, *Macromol. Chem. Phys.* **2011**, *212*, 1719.